ELASTIC AND ACOUSTOELASTIC PROPERTIES OF RAILROAD RAIL

R. B. Thompson, S. J. Wormley, J. C. Johnson
Center for Nondestructive Evaluation
Iowa State University
1915 Scholl Road, ASC-II Building
Ames, IA 50011

David Utrata
Association of American Railroads
3140 S. Federal Street
Chicago, IL 60616

INTRODUCTION

The measurement of thermally induced longitudinal forces in railroad rail is an important element in the control of train damage due to rail buckling or other modes of track failure. Acoustoelastic techniques, whereby stresses are inferred from small shifts in the ultrasonic velocity, are attractive because they can sample the stresses on the interior of the rail and because relatively simple instrumentation can be utilized [1]. The effectiveness of acoustoelastic techniques, however, is limited by the degree to which other sources of velocity shifts are present, generally associated with rail-to-rail variations in microstructure. Figure 1 illustrates the problem. Stress is inferred from the shift in velocity from its stress free value, based on a proportionality constant known as the acoustoelastic constant. Errors in the values of either the stress free velocity or the acoustoelastic constant can lead to errors in the predicted stress.

SAMPLES

Ultrasonic velocity measurements were made on a set of rectangular samples cut from the heads of new and used rail. As shown in Figure 2, these had approximate dimension 1.5" (3.8 cm) x 1.25" (3.2 cm) x 1" (2.5 cm). We define our coordinate system such that the 1, 2, and 3 axes are respectively parallel to the sample axes along which these dimensions are measured, i.e., the length, width, and height of the rail. Table I documents the origin of each sample as well as their total alloy content.

Review of Progress in Quantitative Nondestructive Evaluation, Vol. 14
Edited by D.O. Thompson and D.E. Chimenti, Plenum Press, New York, 1995

$V = V_0 + K\sigma_0$

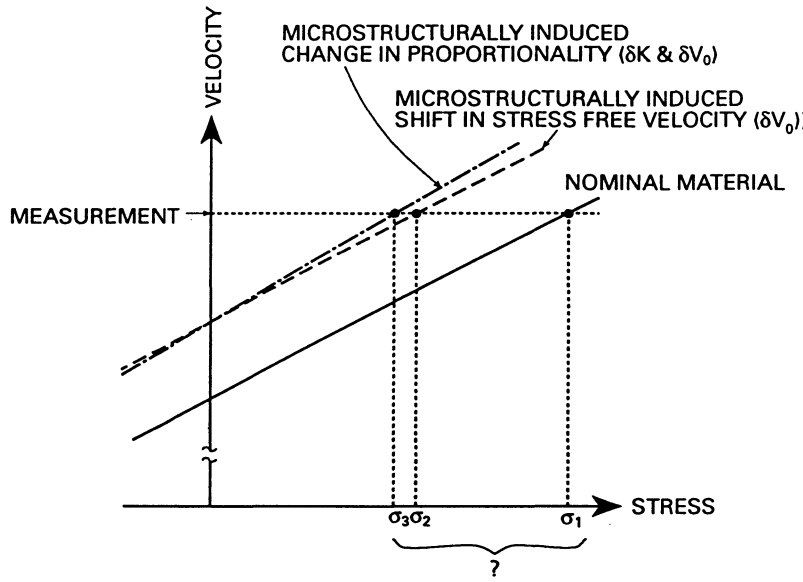

Figure 1 Microstructural sources of uncertainty in the acoustoelastic prediction of stress.

Table I Source of samples.

I. D. Number	Metallurgy	Alloy Wt. %
1	Used Cr-Mo	2.701
2	Wheeling-Pitt Intermediate Strength	2.245
3	Sacilor Stretch-Straightened	2.392
4	Krupp Cr-V	3.518
5	NKK Head Hardened	1.942
6	Algoma Cr-V	3.264
7	Nippon HH Si-Cr	2.802
8	Beth FHT	2.322
9	British 1% Cr	3.499
10	Wheeling-Pitt Cr-Mo	2.544
11	Beth Med. Hard	2.4
12	Beth Standard C	2.215
13	CF&I Cr-Mo	2.654

VELOCITY MEASUREMENTS

The velocities of one longitudinally and two transversely polarized shear waves propagating along the three orthogonal axes of each sample were measured (9 velocities on 13 samples). All measurements were made with 5 MHz, 0.25" (0.64 cm) diameter contact probes, and the velocity was inferred from the difference in the time of a selected zero-crossing in the first and second echo. For the longitudinal wave measurements, this time

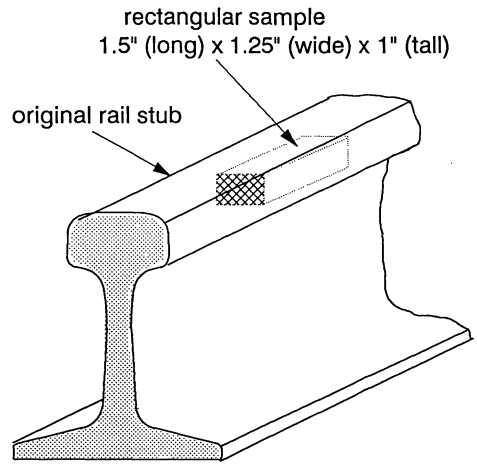

Figure 2 Geometry and location of samples.

was measured with a Hewlett-Packard time averaging counter, with an estimated uncertainty of 0.8 nsec. For the transverse wave measurements, a LeCroy digitizer, with an estimated uncertainty of 2 nsec, was used. Tests for the shear wave measurements indicated a repeatability of 0.1%. No corrections were made for the effects of diffraction.

TEST FOR CONTINUUM RESPONSE

An assumption that underlies all acoustoelastic techniques is that the medium behaves as an anisotropic, elastic continuum. Assuming an orthotropic symmetry, which allows nine independent elastic constants, this implies $V_{ij} = V_{ji}$ where the first subscript denotes the direction of wave propagation and the second denotes the direction of wave polarization. Figure 3 shows the data obtained on all samples, using common symbols for the velocities that would be expected to be equal based on these symmetry considerations. For two sample, numbers 5 and 11, repeat runs were made. These data are plotted as the results for sample numbers 5.5 and 11.5. The greatest difference between velocities expected to be equal on the basis of symmetry was 0.28% for sample 2. Although outside the difference of 0.2% expected on the basis of the repeatability estimate, the 0.28% difference seems sufficiently close to that estimate to be reasonably explained by experimental uncertainty. Pending more precise measurements, the evidence suggests that modeling the medium as an anisotropic elastic continuum is a good approximation.

ANISOTROPY

The data in Figure 3 also illustrate that there is a significant anisotropy present. Figure 4 reinterprets this in terms of the shear wave birefringence that exists for waves propagating along the three principal directions. Considerable rail-to-rail variation can be seen. Sample 4 is nearly isotropic ($\frac{\Delta V}{V} < 0.05\%$ in any direction) while samples 2 and 12 have the largest anisotropies. For example, the latter two have birefringences ($\frac{\Delta V}{V}$) of

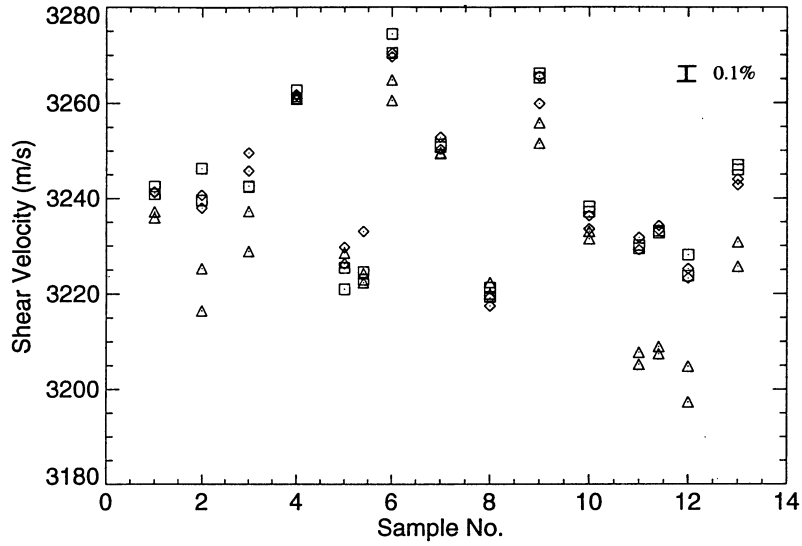

Figure 3 Ultrasonic shear velocities on all samples, plotted to emphasize symmetry, common symbols denote velocities expected to be equal since they are governed by the same elastic constant: Δ-C_{44},◇-C_{55}, □-C_{66}.

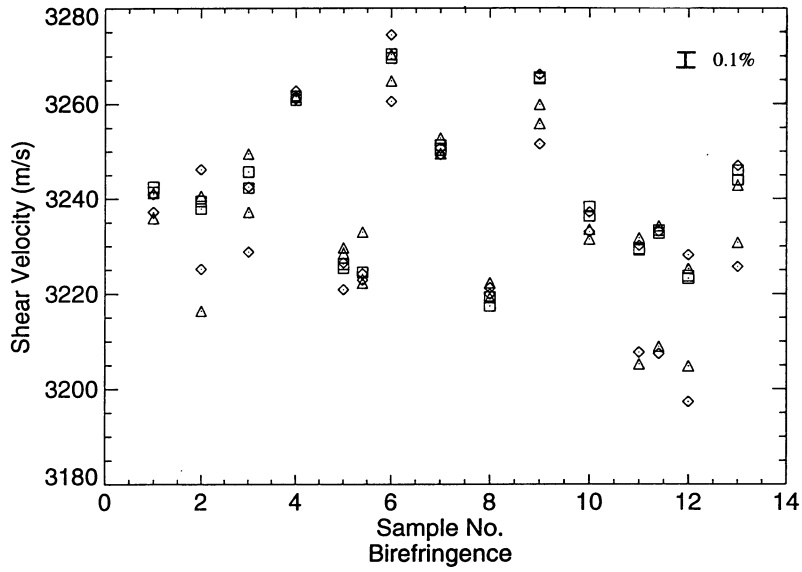

Figure 4 Ultrasonic shear velocities on all samples, plotted to emphasize birefringence. Common symbols denote velocities of waves propagating in the same direction: □-1, ◇-2, Δ-3.

0.75% and 0.64% respectively for waves propagating from top to bottom (3-direction). The existence of this variable anisotropy is a major challenge to the implementation of the shear wave birefringence technique for stress measurement in the field.

Figure 5 compares the velocities of longitudinal waves traveling in the three directions in each of the 13 samples. It can be seen that these exhibit similar degrees of anisotropy.

VELOCITY COMBINATIONS

Allen et al. showed that, for aggregates of cubic crystallites, the following relationship holds

$$\left[V_{i1}^2 + V_{i2}^2 + V_{i3}^2\right] = (\lambda + 4\mu)/\rho \qquad (1)$$

where λ and μ are the Lame constants that would be observed in the absence of texture [2,3]. This implies that the sums of the velocities in any direction of a given rail should be equal. Figure 6 presents the indicated sums of the squares of the observed velocities for the 13 samples. Since these sums do not appear to be totally independent of propagation direction, the result suggests that the velocity combinations technique prepared by those investigators would not be applicable to railroad rail. It is our speculation that this result is a consequence of the orthorhombic Fe_3C phase present in the pearlitic microstructure of railroad steel.

EFFECTS OF COMPOSITION

Examination of the above data reveals considerable rail-to-rail variation in average velocity as well as anisotropy. In Figures 7 and 8 the longitudinal and shear wave data is plotted as a function of alloy weight percent. A systematic increase in average velocity with alloy weight percent is observed, which appears to explain a significant amount of the rail-to-rail variation.

ACOUSTOELASTIC CONSTANT

Measurements of the acoustoelastic constants are in progress. Preliminary results are consistent with the range of values reported by Hirao et al [4].

CONCLUSIONS

The measurement of stress (and hence longitudinal force) in railroad rail depends on knowledge of the stress free velocities and acoustoelastic constants of the material. Measurements on samples from 13 rails typical of those used in the United States exhibit considerable rail-to-rail variation in average velocity and anisotropy, with the former being partially explained by compositional variations. These velocity shifts are comparable to or greater than the shifts due to stress. Therefore, any stress measurement technique proposed for the field must include a strategy for dealing with those effects. It is hoped that this data will provide a data base which will assist in developing those strategies.

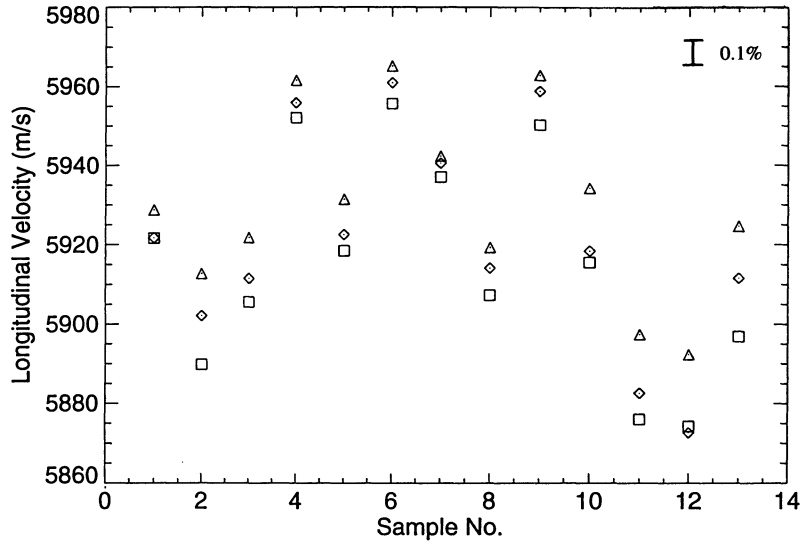

Figure 5 Longitudinal velocity on all samples for each propagation direction: □-1, ◇-2, Δ-3.

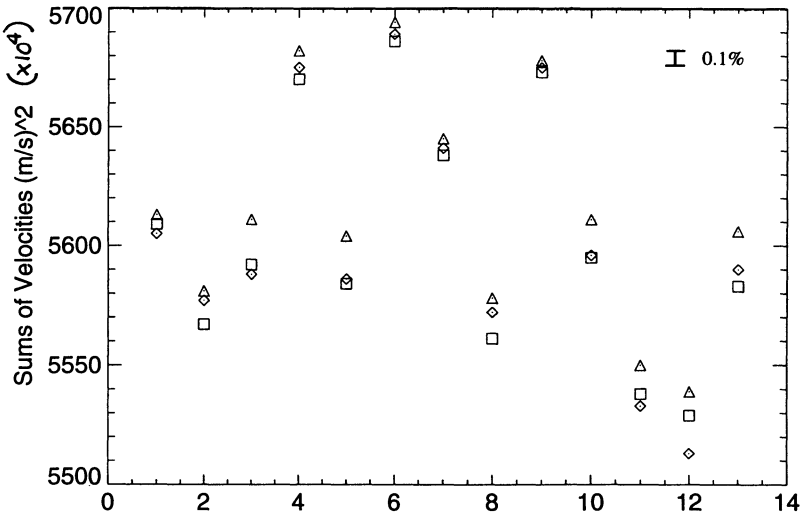

Figure 6 Sum of squares of velocities of three waves propagating in a common direction on all samples: □-1, ◇-2, Δ-3.

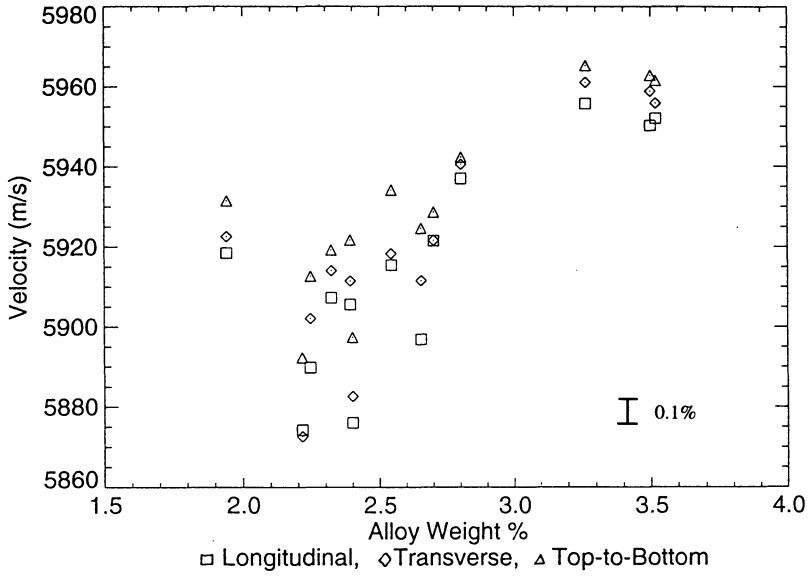

Figure 7 Longitudinal velocity as a function of total alloy weight % in each direction: □-1, ◇-2, Δ-3.

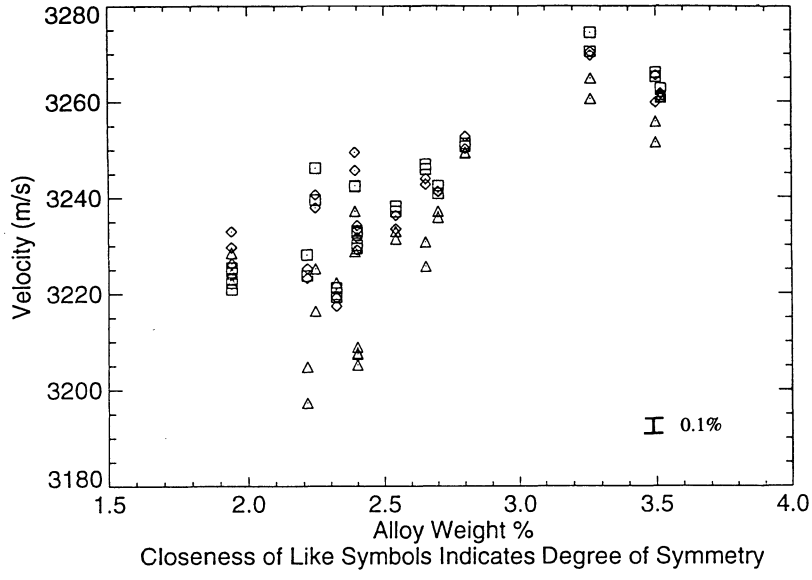

Figure 8 Shear wave velocity as a function of total alloy weight %. Common symbols denote velocities expected to be equal by symmetry, using the same symbols as Figure 3.

ACKNOWLEDGEMENT

This work was supported by the NSF Industry/University Center for NDE at Iowa State University.

REFERENCES

1. R. B. Thompson, W.-Y. Lu, A. V. Clark, Jr., "Ultrasonic Methods", in SEM Monograph on Techniques for Residual Stress Measurement (SEM, in press).
2. D. R. Allen, W. M. B. Cooper, C. M. Sayers, and M. G. Silk, "The Use of Ultrasonics to Measure Residual Stress", in Research Techniques in Nondestructive Testing, Vol. VI, Edited by R. S. Sharpe (Academic Press, NY, 1982), pp. 51-209.
3. D. R. Allen and C. M. Sayers, "The Measurement of Residual Stress in Textured Steel Using an Ultrasonic Velocity Combinations Techniques", Ultrasonics 22, 179 (1984).
4. M. Hirao, H. Ogi and H. Fukuoka, "Advanced Ultrasonic Method for Measuring Rail Axial Stresses with Electromagnetic Acoustic Transducers", Res. Nondestr. Eval. 5, 211-223 (1994).